NUSC Technical Document 5234

12 NW

An Adaptive Kalman Filter Tracker for Multi-mode Range/Doppler Sonar

C. Nicholas Pryor
Technical Director

5 March 1977

NAVAL UNDERWATER SYSTEMS CENTER
Newport Laboratory

PREFACE

The information contained in this document was initially presented at the NATO Advanced Study Institute on Signal Processing, held September 1976 at Portovenere (La Spezia) Italy.

The contribution of Mr. Ed Hug of the SACLANT Center is gratefully acknowledged. Certain of the ideas presented in this work, particularly in the area of adaptive control, resulted from discussions held with Mr. Hug during the last meeting of the Institute in Loughborough, England.

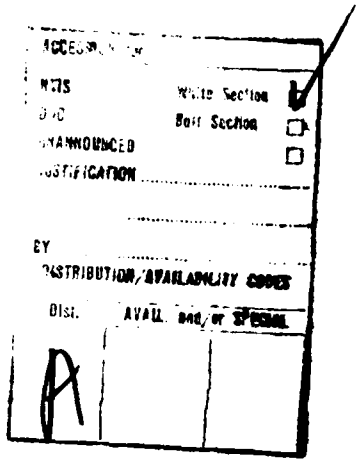

REVIEWED AND APPROVED: 5 March 1977

C. Nicholas Pryor

C. Nicholas Pryor
Technical Director

The author of this document is located at the Newport Laboratory, Naval Underwater Systems Center, Newport, Rhode Island 02840.

UNCLASSIFIED

SECURITY CLASSIFICATION OF THIS PAGE (When Data Entered)

REPORT DOCUMENTATION PAGE	READ INSTRUCTIONS BEFORE COMPLETING FORM
1. REPORT NUMBER: TD 5234 ✓	2. GOVT ACCESSION NO. / 3. RECIPIENT'S CATALOG NUMBER
4. TITLE (and Subtitle): AN ADAPTIVE KALMAN FILTER TRACKER FOR MULTI-MODE RANGE/DOPPLER SONAR,	5. TYPE OF REPORT & PERIOD COVERED: Technical Report
	6. PERFORMING ORG. REPORT NUMBER
7. AUTHOR(s): C. Nicholas Pryor	8. CONTRACT OR GRANT NUMBER(s)
9. PERFORMING ORGANIZATION NAME AND ADDRESS: Naval Underwater Systems Center ✓ Newport Laboratory Newport, Rhode Island 02840	10. PROGRAM ELEMENT, PROJECT, TASK AREA & WORK UNIT NUMBERS
11. CONTROLLING OFFICE NAME AND ADDRESS: [illegible]	12. REPORT DATE: 5 March 1977 / 13. NUMBER OF PAGES: 20
14. MONITORING AGENCY NAME & ADDRESS (if different from Controlling Office): [illegible]	15. SECURITY CLASS. (of this report): UNCLASSIFIED / 15a. DECLASSIFICATION DOWNGRADING SCHEDULE

16. DISTRIBUTION STATEMENT (of this Report)

Approved for Public Release; Distribution Unlimited.

17. DISTRIBUTION STATEMENT (of the abstract entered in Block 20, if different from Report)

18. SUPPLEMENTARY NOTES

19. KEY WORDS (Continue on reverse side if necessary and identify by block number)

Kalman Filtering
Acoustic Signal Processing
Fire Control System Target Motion Analysis
Adaptive Control Techniques

20. ABSTRACT (Continue on reverse side if necessary and identify by block number)

This document presents the use of Kalman filter methods for making optimum use of incoming range and doppler information in determining a target track. Specifically, it (1) illustrates the fundamental application of linear Kalman filter mathematics; (2) expands the matrix equations to show the form and characteristics of the filter; (3) shows two methods of making the filter adaptive to target maneuvers through use of statistical properties of the measurement residuals; and (4) presents a means of using the

DD FORM 1 JAN 73 1473 EDITION OF 1 NOV 65 IS OBSOLETE
S/N 0102-014-6601

UNCLASSIFIED 406 068
SECURITY CLASSIFICATION OF THIS PAGE (When Data Entered)

20. Abstract (cont'd)

uncertainty matrix of the tracker to select the optimum waveform for the subsequent ping, when the desire is to minimize the range error at some future time.

TABLE OF CONTENTS

LIST OF ILLUSTRATIONS

AN ADAPTIVE KALMAN FILTER TRACKER FOR MULTI-MODE RANGE/DOPPLER SONAR

INTRODUCTION

In most modern sonar systems, each active ping produces a combination of information on both the range and the range rate of the target. This information is then used to form the basis of a target track. This document presents the use of Kalman filter methods to make optimum use of the incoming range and doppler information in forming the track. The first part of the discussion shows the fairly routine application of linear Kalman filter mathematics, and expands the matrix equations to show the actual form of the filter and some of its characteristics. Two methods are then discussed for making the filter adaptive to target maneuvers through use of statistical properties of the measurement residuals. Finally, a means is described for using the uncertainty matrix of the tracker to select the optimum waveform for the next ping, when the desire is to minimize the range error at some future time.

DISCUSSION

The steps required in defining a Kalman filter problem involve first describing the state vector X to be estimated, modeling the dynamic evolution and the random processes influencing this state vector, and then describing the relationship between this state vector and the measurements being made on it, along with the uncertainty in these measurements. For the problem at hand, we will estimate the range and the range rate of the target. Thus, the state vector X becomes

$$X = \begin{matrix} x_1 \\ \\ x_2 \end{matrix} \Bigg] = \begin{matrix} \text{range in meters} \\ \\ \text{range rate in meters/second} \end{matrix}$$

In describing the evolution of this state vector, we wish to show that the range is the integral of the range rate and that the range rate is influenced randomly by target maneuvers. This can be done by writing

$$\dot{x}_1 = x_2$$

$$\dot{x}_2 = (w - x_2)/\tau$$

where the differential equation for x_2 causes it to behave as a low-pass process with relaxation time τ with w as a white noise excitation. Thus, the range rate will evolve from its current value toward some new unknown value described only by its variance, in a time on the order of τ seconds. Putting this into the matrix notation of continuous Kalman filters gives

$$\dot{X} = F X + G w$$

where

$$F = \begin{bmatrix} 0 & 1 \\ 0 & -1/\tau \end{bmatrix} \quad \text{and} \quad G = \begin{bmatrix} 0 \\ 1/\tau \end{bmatrix} .$$

Now given this information on the dynamics of the process, it can be shown that the uncertainty matrix P on the estimate of the state evolves according to the differential equation

$$\dot{P} = F P + P F^t + G Q G^t$$

where Q is the power density of the noise process w. Expanding this matrix equation for the three components of P gives

$$\dot{P}_{11} = 2 P_{12}$$

$$\dot{P}_{12} = P_{22} - P_{12}/\tau$$

$$\dot{P}_{22} = -2 P_{22}/\tau + Q/\tau^2$$

The above differential equations are simple enough to be integrated to show the evolution in both the best state estimate and in the uncertainty matrix from a time t_o to a new time t.

These results are

$$x_1(t) = x_1(t_o) + \alpha \tau x_2(t_o)$$

$$x_2(t) = (1-\alpha)x_2(t_o)$$

$$P_{11}(t) = P_{11}(t_o) + 2\alpha\tau P_{12}(t_o) + \alpha^2\tau^2 P_{22}(t_o) + \left[2(t-t_o)/\tau - 2\alpha - \alpha^2\right] \tau^2 V^2$$

$$P_{12}(t) = (1-\alpha) P_{12}(t_o) + \alpha(1-\alpha)\tau P_{22}(t_o) + \alpha^2\tau V^2$$

$$P_{22}(t) = (1-\alpha)^2 P_{22}(t_o) + \alpha(2-\alpha) V^2$$

where

$$\alpha = 1 - \exp(-(t-t_o)/\tau)$$

and $V^2 = Q/2\tau$ has been introduced as the value toward which the mean squared range rate uncertainty evolves.

It is interesting to look at these equations both for prediction times short compared to τ, where $\alpha \approx (t-t_o)/\tau$, and for long prediction times where α approaches unity. In the short time limit, these equations may be reduced by dropping higher order terms in $t-t_o$ to those which are obtained if a discrete model of the process were used. In the long time limit the range rate uncertainty P_{22} evolves from $P_{22}(t_o)$ toward the a priori uncertainty in velocity V^2. The covariance term P_{12} evolves toward the constant τV^2, which indicates that the range error and range rate error in the estimates will eventually be positively correlated. The range uncertainty P_{11} has perhaps the most interesting characteristic. This uncertainty contains a term contributed by each of the initial components of the uncertainty matrix, and each of these terms approaches a constant. In addition, there is a term which eventually increases linearly with time and is proportional to the variance of the target velocity and to its relaxation time.

It is now necessary to describe the process by which new measurement data are inserted into the filter. This is a discrete process and is described by a measurement matrix H giving the relationship between the measured parameters and state vector of the filter. Since the measured information from each ping is also range and range rate, it would seem that the relation between the state vector and the measurement is trivial. However, this is not so because of the acoustic propagation time delay involved. The measurement is taken at the time the signal reflects from the target, but is not available at the tracker input until the signal returns to the sonar. If an attempt is made to maintain the track directly in current time, a term of the form $x_1 - x_1x_2/c$ appears in the measurement equations and causes the tracker to be nonlinear. This complication can be eliminated by developing the tracker in the form shown in figure 1. The first part is the actual Kalman filter, and it is updated

once per ping cycle with a new state vector X, a new uncertainty matrix P, and a time representing the time of reflection of the last echo. This time is computed by subtracting the one-way travel time at the estimated range from the actual time of receipt. While this technique does not completely eliminate the nonlinearity, because of the uncertainty in the range estimate, it does reduce it to second order.

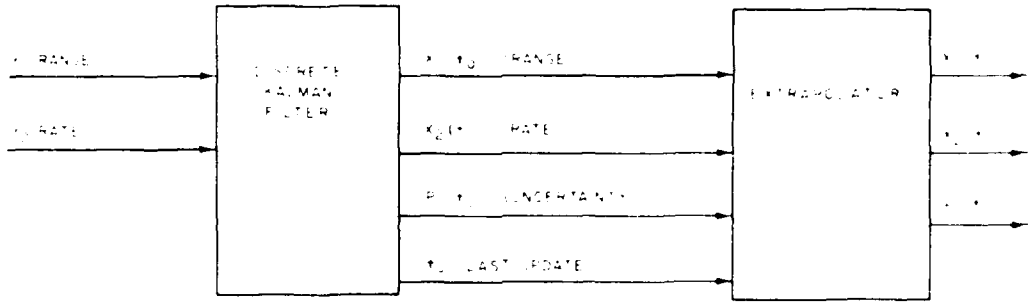

Figure 1. Configuration of the Kalman Filter

In most cases a range estimate is desired more frequently than once per ping cycle. Thus, a second element is shown in figure 1, which uses the most recent information in the Kalman filter to provide a current (or future) estimate for X, and if desired for the estimated uncertainty P. With this technique the measured parameters become identical to the state parameters, so the measurement matrix H is simply a unit matrix. The error matrix for the measurement is a 2 by 2 matrix R.

With this definition of the problem, the process for updating the Kalman filter estimate involves first computing the new update time t by subtracting the one-way travel time from the time of echo reception (or adding it to the time of transmission). The state estimates and the P matrix are then updated to that time. The process of inserting the new data involves first computing a Kalman gain matrix of the form

$$K = P\,H^{t}\left[H\,P\,H^{t} + R\right]^{-1} \quad ,$$

which is multiplied by the vector of measurement residuals Y - H X to map them into corrections to the state vector in the form

$$X = X + K\left[Y - H X\right] \quad .$$

The K coefficients thus represent the relative weights attached to the new measurement as compared to the previous estimate. Finally, the P matrix is adjusted according to the equation

$$P = P - K H P$$

to represent the reduction in uncertainty due to the introduction of the new data.

Since the H matrix has been found to be a unit matrix, we can expand these equations in terms of the P matrix at the time of the echo and the R matrix associated with the ping waveform to give

$$K_{11} = \left[P_{11}(P_{22} + R_{22}) - P_{12}(P_{12} + R_{12})\right] / \left[(P_{11} + R_{11})(P_{22} + R_{22}) - (P_{12} + R_{12})^2\right]$$

$$K_{12} = (P_{12}R_{11} - P_{11}R_{12}) / \left[(P_{11} + R_{11})(P_{22} + R_{22}) - (P_{12} + R_{12})^2\right]$$

$$K_{21} = (P_{12}R_{22} - P_{22}R_{12}) / \left[(P_{11} + R_{11})(P_{22} + R_{22}) - (P_{12} + R_{12})^2\right]$$

$$K_{22} = \left[P_{22}(P_{11} + R_{11}) - P_{12}(P_{12} + R_{12})\right] / \left[(P_{11} + R_{11})(P_{22} + R_{22}) - (P_{12} + R_{12})^2\right]$$

for the Kalman gain equations,

$$x_1 = x_1 + K_{11}(y_1-x_1) + K_{12}(y_2-x_2)$$

$$x_2 = x_2 + K_{21}(y_1-x_1) + K_{22}(y_2-x_2)$$

for the state vector corrections, and

$$P_{11} = (1-K_{11})\ P_{11} - K_{12}P_{12}$$

$$P_{12} = (1-K_{11})\ P_{12} - K_{12}P_{22}$$

$$P_{22} = (1-K_{22})\ P_{22} - K_{21}P_{12}$$

for the adjustments to the P matrix. Note that the differences between the observed and predicted values of both range and range rate are used in correcting both state estimates, as desired. The Kalman gains tend to be ratios of variances. In a simple example, if both P_{12} and R_{12} were zero, K_{11} becomes $P_{11}/(P_{11} + R_{11})$ or the variance of the range estimate divided by the variance of the measurement residual, as might have been expected. Note that for any cross-coupling to occur between the range and range rate estimates, either P_{12} or R_{12} must be non-zero. However, as we have seen earlier, the P_{12} covariance term will always evolve toward a positive non-zero value.

As shown before, the terms of the P matrix tend to increase between measurements due to the random process assumed in the model, while it is seen here that the measurement process tends to decrease the P matrix. Normally, if measurements are taken on a regular basis these two effects balance to give stable values to the P matrix. These effects point up the need for the random perturbations in the target model. If they were not included, the P matrix would tend to zero, causing all the Kalman gain terms to go to zero. The filter would then no longer respond to new measurements, being satisfied that it knew all there was to know about the target. This

is the malfunction known as divergence in Kalman filter literature.

A simulated example of the performance of this Kalman filter is based on the target track shown in figure 2a. The target proceeds inbound at 10 meters/second (about 20 knots) from a range of 10 kilometers to a range of 5 kilometers. It then makes a 90-degree turn at 3 degrees per second and again proceeds in a straight line. This track, translated into a trajectory in range/range rate space, is shown in figure 2b. Sonar data is assumed to come from a sonar operating at 5 kiloHertz with a 100 millisecond Continuous Wave (CW) pulse. A pulse is transmitted immediately after each echo is received, giving an interpulse interval of 6.5 to 13 seconds, depending on range. While the measurement uncertainty in an echo strictly depends on signal-to-noise ratio, this dependency is ignored here and the standard deviations in the echo measurement are assumed to be 100 milliseconds in time and 10 Hertz in doppler. This is equivalent to 75 meters in range and 1.5 meters/second in range rate, and these two errors are uncorrelated.

The most interesting part of the track is the shaded area of figure 2b, extending from just before the turn until the target range and range rate again begin to change significantly. This region is shown enlarged in figure 3a, with the actual target track shown by the solid curve and the measured data shown by the open circles connected by the dotted lines. Since the measurement error is large compared to the target motion between pings, smoothing of the data is required in order to form a sensible target track. Actual rms error of range samples in the 20 pings before the maneuver was 67.4 meters, while the actual rms error in range rate samples was 1.45 meters/second. Performance of various forms of the Kalman filter will be compared in terms of the amount of smoothing of these data points during steady-state conditions and by the general nature of the response to the maneuver.

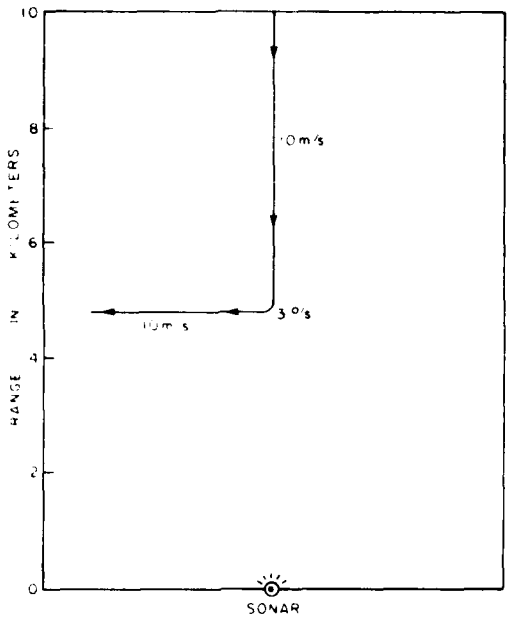

Figure 2a. Geometry of Simulated Run

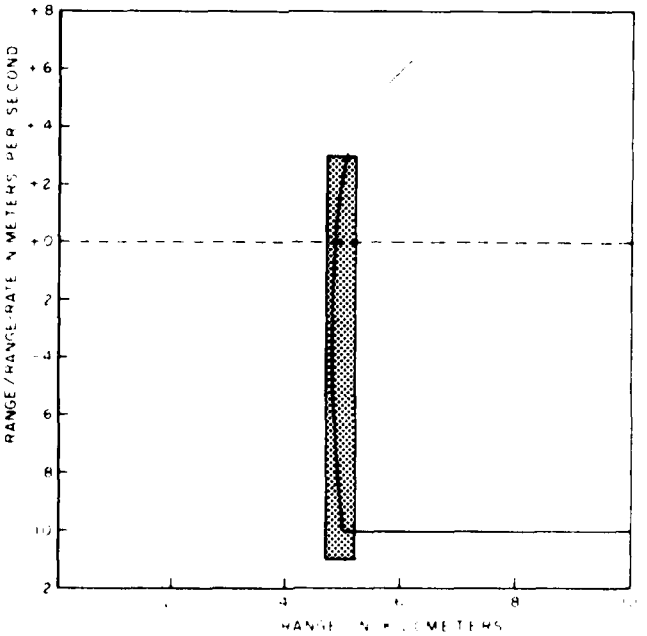

Figure 2b. Range / Range Rate Trajectory of Simulated Run

Figure 3b shows the data as tracked by the Kalman filter; an arbitrarily selected relaxation time τ of 300 seconds is used. Each circled dot represents the output of the filter immediately after a ping is received, while the straight line is the prediction from that point until the next ping, as would be performed by the second block in figure 1. During the steady-state portion of the track, rms range error was reduced to 19.65 meters, or a factor of about 3.5. Rms range rate error was reduced to 1.11 meters/second, or only slightly below that of the input data. Response during the maneuver was good, primarily as a result of the limited smoothing of range rate data. Since the relaxation time τ determines the steady-state values of the P matrix, selection of this parameter determines the effective filter time constants and thus the balance between smoothing and responsiveness. Significantly larger τ would improve the smoothing, but at the expense of responsiveness to the maneuver. Note that the rate estimate stays nearly constant between pings, and there is no tendency for it to predict the actual range rate changes during the maneuver. This is due to the two-state model used; any prediction of range rate would require addition of a third acceleration variable to the state vector.

It is interesting to compare this track with one obtained using only the range data from each ping and ignoring the range rate data obtained from echo doppler. This track is shown in figure 3c. The rms range error during the straight-line portion of the track was 38.40 meters, or about double the error obtained when the rate data was included. The rms range rate error, derived entirely from the range samples, was 1.82 meters/second, which is inferior to the samples of the input rate data. This form of the Kalman filter, estimating range and rate from range data only, is equivalent to the "α, β tracker" often used in radar systems.

As mentioned previously, the smoothing performance of the Kalman filter tracker shown can be improved by increasing the assumed value of τ, but the response to maneuvers eventually becomes unacceptable. This conflict can be

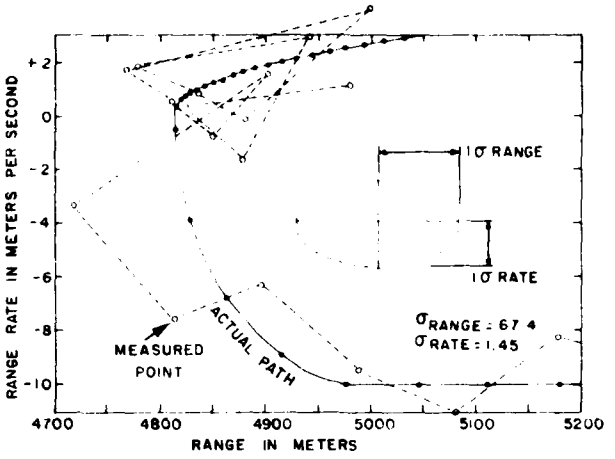

Figure 3a.
Raw Measurement Data Points

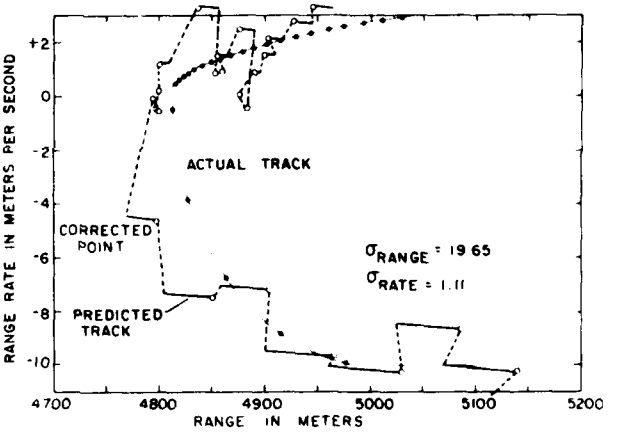

Figure 3b.
Kalman Filter Tracker Output
(τ= 300 sec)

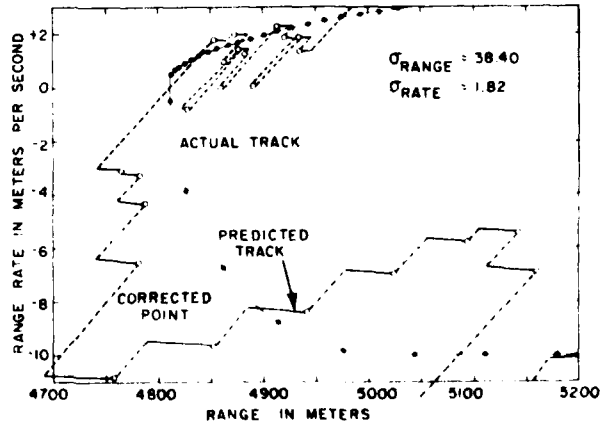

Figure 3c.
Kalman Filter Output with
Range Data Only (τ= 300 sec)

overcome by attempting to sense target maneuvers and adapting the parameters of the filter to them. This is rather easy to do with a Kalman filter, based on the fact that the scalar function

$$z = [Y-HX]^t \; [\, HPH^t+R\,]^{-1} \; [Y-HX]$$

is a normalized chi-squared random variable with degrees of freedom equal to the size of the measurement vector, when the target and measurement data are properly modeled. If this statistic is formed for each data sample, it may be tested against a threshold to determine whether the input data residuals are reasonably explainable as random errors. If an abnormally large value of z occurs, it may be used as a signal that the target has maneuvered and that we wish to increase the responsiveness of the filter. Two simple ways of implementing this will be illustrated: the first using samples of z to adapt the parameter τ to the target behavior, and the second operating directly on the P matrix.

Adaptation in τ is performed by continually increasing τ (decreasing the assumed maneuvers of the target) as long as z does not exceed a threshold, and decreasing τ whenever a large value of z suggests that the target may be maneuvering faster than the model assumed. This can be done in rather crude ways, since changes in τ only affect the rate of growth of the P matrix which, in turn, determines the Kalman gains. Figures 3d and 3e show the performance of two trackers using adaption in τ. In the first case, a threshold z_0 was set at the median value 1.386 of the chi-squared variate, and τ was doubled whenever z fell below, and cut in half when z exceeded z_0. With this approach, one would expect τ to stabilize around a value consistent with the random maneuvers of the target. During the straight-line portion of the example run, τ did increase to very large values consistent with the non-maneuvering target. This was reflected in additional smoothing of the input data, particularly in range rate. The rms range-rate error at the tracker output was 0.37 meters/second, or about a

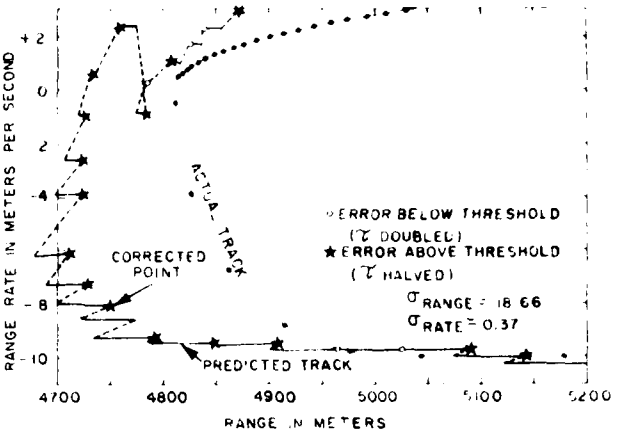

Figure 3d.
τ-Adaptive Kalman Filter Output

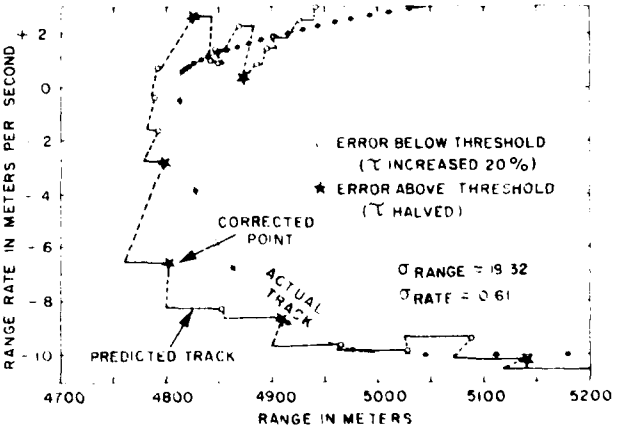

Figure 3e.
τ-Adaptive Kalman Filter Output

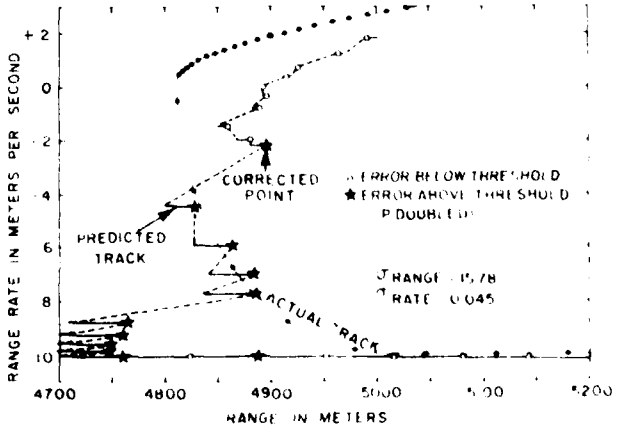

Figure 3f.
P-Adaptive Kalman Filter Output

third that of the non-adaptive tracker, while the range error was not significantly different from the non-adaptive case. Once the maneuver started, it was detected immediately by the z statistic test. However, the filter output did lag significantly in both range and rate while the τ values were being reduced enough to affect the P matrix, and therefore, the input data weightings.

Figure 3e shows the somewhat different performance obtained when the threshold z_o was changed to the 80 percentile point, 3.219, on the chi-square distribution. In this case τ was increased by only $\sqrt[4]{2}$ or about 20 percent when z was below z_o, but still was cut in half when z exceeded the threshold. This still causes τ to seek the proper long-term value but to increase less rapidly during non-maneuvering periods. This led to a more responsive track when the maneuver occured in the example, but at the expense of an increase in the rate tracking error during the straight-line segment.

The second method of adaptation has less to do with the physical model of the target but is also quite effective. This technique simply increases the value of the P matrix (which essentially means that less is known about the state of the target than first believed) whenever z exceeds a threshold. Since each new measurement tends to decrease the P matrix anyway, it is not necessary to reduce the P matrix when z falls below the threshold. It is possible to make <u>selective</u> increases in the P matrix whenever a simple relation exists between the state variables and the measured data, for example, increasing both the row and column corresponding to a given variable whenever its residual exceeds a threshold. However, in the example shown in figure 3f, the entire P matrix is simply doubled whenever z exceeds the 95 percentile point, 5.991. Since the P adaptation provides a means of increasing the P matrix, the random excitation in the target model was removed. This made the model correspond to a non-maneuvering target and left the adaptive mechanism as the only means of avoiding divergence in the

filter. Note that during the straight-line portion of the track the rms range rate error was only 0.045 meters/second, reduced about a factor of 30 from the error of the input data. However, because the P_{22} term of the P matrix gets quite small, the filter is slow to respond to changes in the range rate even after the maneuver is detected. This could be avoided by keeping a small randomness in the target model to limit the smoothing of the range rate data.

While neither of the methods of adaption discussed here completely reaches the goal of an optimum track for both maneuvering and non-maneuvering targets, both are quite simple to implement and provide some performance improvement. In a practical application, one or the other (or perhaps a combination of the two) could provide useful improvements over non-adaptive trackers.

A second interesting use can be made of the P matrix information in the Kalman filter. As we have seen earlier, the P matrix can be projected into the future to show the state of target uncertainty at some future time, assuming no more information is gained from the sonar. This in itself is tactically useful. We can also estimate the effect of an additional sonar ping by projecting the P matrix to the predicted time of the echo, adjusting it to account for the information expected from that echo, and then continuing the projection on into the future. This can be used as an algorithm for selecting ping waveforms in a multimode sonar.

Suppose there is some time in the future, such as the expected time of arrival of a weapon, at which the target range should be known as accurately as possible. By carrying out the above process for each of the available ping waveforms, the expected future range uncertainties can be compared and the waveform giving the lowest value for P_{11} selected. The form of the previously shown equation for $P_{11}(t)$ shows the intuitive result of this process. The portion of this expression which can be affected by the ping waveform selected is $P_{11}(t_o) + 2(\alpha\tau)P_{12}(t_o + (\alpha\tau)^2 P22(t_o)$. As long as the

projection is far into the future so that $\alpha\tau$ is large, it is important to minimize $P_{22}(t_o)$ and waveforms with good doppler resolution will tend to be preferred. Once the projection time becomes short, however, the $P_{11}(t_o)$ term becomes the most important and waveforms with good range resolution will tend to be selected. It is also clearly an advantage to make $P_{12}(t_o)$ as negative as possible, which leads to a preference for waveforms with large negative $P_{12}(t_o)$.

Consider, as an example, a sonar with the option of either continuous wave (CW) or upward or downward linear FM transmissions. As before, we will assume for a ping duration of T seconds that the time (range) measurement variance of the CW signal is T^2 and the variance of the frequency (range rate) measurement is $1/T^2$ with no correlation between them and independent of signal-to-noise ratio. Figure 4 shows how the R matrix is derived for the linear FM signals, by means of the familiar ambiguity function for such signals. The mean square range error when doppler is unknown is still T^2, but this value reduces to $1/W^2$ when the target doppler is known. Similarly, the variance in frequency when range is unknown is W^2, while it becomes $1/T^2$ when the range is known. Since the diagonal terms of the R covariance matrix are the variances of the marginal error distributions, and since the conditional variances are smaller than the marginal variances by the factor $1 - R_{12}^2/R_{11}R_{22}$, we find that for a linear FM signal the R matrix is of the form

$$\begin{bmatrix} R_{11} & R_{12} \\ R_{21} & R_{22} \end{bmatrix} = \begin{bmatrix} T^2 & \pm\sqrt{W^2T^2-1} \\ \pm\sqrt{W^2T^2-1} & W^2 \end{bmatrix}$$

where the plus sign applies for upward FM signals while the minus sign applies for downward FM signals.

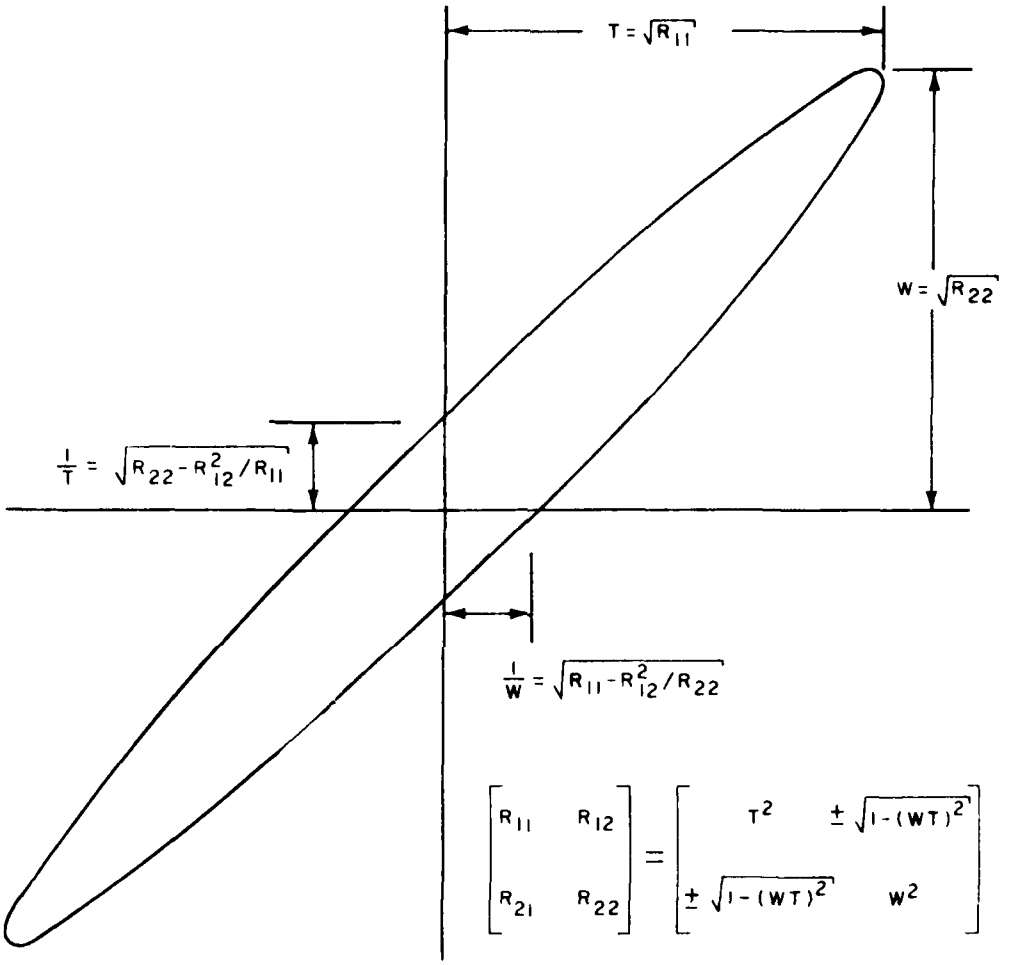

Figure 4. Ambigutiy Matrix for Linear FM Signal

Limited simulation experiments with such a sonar confirm that when the objective time, at which the range error is to be minimized, is well into the future the CW mode is invariably selected because of its better range rate accuracy. As the objective time approaches, the sonar finally switches to a down-slope FM signal to take advantage of its conditional range accuracy. The down-slope is preferred to the up-slope FM because the

range rate error tends to be in a direction to reduce the range error at a future time. If all parameters of the problem were known in advance, it appears that one could pre-compute the optimum time to switch from CW to FM transmissions. However, if this technique is to be combined with adaption or with compensation for observed signal-to-noise ratios, it may be an advantage to do the waveform selection computations in real time on each ping.

SUMMARY

This document has presented the application of Kalman filter techniques to range and doppler tracking in active sonar systems. The Kalman filter inherently provides an uncertainty matrix, which indicates the accuracy of the solution. This uncertainty matrix formation can also be used to provide adaptive operation and to aid in waveform selection in multi-mode sonars.

INITIAL DISTRIBUTION LIST

Addressee	No. of Copies
NAVSEA (SEA-034; -660, Dr. Snuggs)	2
ASWSPO (ASW-13)	1
NADC, Warminster (Library; J. Howard)	2
NWC, China Lake (Library)	1
NSRDC, Bethesda (Library)	1
NCSL, Panama City (Library)	1
NSWC, White Oak (Library; WU-22)	2
NELC, San Diego (Library)	1
NUC, San Diego (Library)	1
NPGS, Monterey (Library)	1
DDC, Alexandria	12
Office of the Science Advisor (CTF 67, P. Nadeau)	1